PHYSICAL REVIEW B **69**, 140503(R) (2004)

Coherent dynamics of a Josephson charge qubit

T. Duty,* D. Gunnarsson, K. Bladh, and P. Delsing
Microtechnology and Nanoscience, MC2, Chalmers University of Technology, S-412 96 Göteborg, Sweden
(Received 10 May 2003; revised manuscript received 31 October 2003; published 5 April 2004)

We have fabricated a Josephson charge qubit by capacitively coupling a single-Cooper-pair box (SCB) to an electrometer based upon a single-electron transistor (SET) configured for radio-frequency readout (rf-SET). Charge quantization of $2e$ is observed and microwave spectroscopy is used to extract the Josephson and charging energies of the box. We perform coherent manipulation of the SCB by using very fast dc pulses and observe quantum oscillations in time of the charge that persist to $\simeq 10$ ns. The observed contrast of the oscillations is high and agrees with that expected from the finite E_J/E_C ratio and finite rise time of the dc pulses. In addition, we are able to demonstrate nearly 100% initial charge state polarization. We also present a method to determine the relaxation time T_1 when it is shorter than the measurement time T_{meas}.

DOI: 10.1103/PhysRevB.69.140503 PACS number(s): 85.25.Hv, 74.40.+k, 85.35.Gv

Although a large number of physical systems have been suggested as potential implementations of qubits, solid-state systems are attractive in that they offer a realistic possibility of scaling to a large number of interacting qubits. Recently there has been considerable experimental progress using superconducting microelectronic circuits to construct artificial two-level systems. A variety of relative Josephson and Coulomb energy scales have been used to construct qubits based upon a single-Cooper-pair box[1,2] and flux qubits based upon a three-junction loop.[3,4] Coherence times of the order of 0.5 μs have been achieved for a single-Cooper-pair box qubit.[2] Rabi oscillations between energy levels of a single large tunnel junction have also been observed.[5,6] Despite the encouraging results, one aspect that is not well understood concerns the contrast of the oscillations, which in all previously reported experiments is smaller than expected.

The experimental systems reported so far can also be distinguished by the readout method and the manner of performing single-qubit rotations. The first demonstration of coherent control of a single-Cooper-pair box[1] (SCB) employed a weakly coupled probe junction to determine the charge on the island. In the more recent experiment reported by Vion *et al.*,[2] the SCB was incorporated into a loop containing a large tunnel junction, for which the switching current depends on the state of the SCB. Switching current measurements of superconducting quantum-interference devices (SQUID's) have also been used for flux and phase-type qubits.[3–6] Nakamura *et al.*[1] performed single-qubit rotations by applying very fast dc pulses to a gate lead in order to quickly move the SCB into and away from the charge degeneracy point. This technique produces qubit rotations with an operation time that can be of the order of the natural oscillation period. Other experiments utilize microwave pulses to perform NMR-like rotations of the qubit.[2,4–6] The latter approach requires less stringent microwave engineering, since rf rotations can be accomplished with pulses that are more than an order of magnitude slower in rise time and duration than the natural oscillation period. By using fast pulses, however, single-qubit rotations can be performed ≈ 20 times faster than with rf rotations.

In this Rapid Communication, we report measurements made on a SCB-type qubit with very fast dc pulses used to effect the qubit rotations, as in Nakamura *et al.*[1] For our qubit, however, the readout system consists of a single-electron transistor (SET) capacitively coupled to the SCB and configured for radio-frequency readout (rf-SET). By incorporating a SET into a tank circuit, rf-SET electrometers can be made that are both fast[7] and sensitive,[8] and are well suited for SCB-qubit readout.[9,10] One advantage of using rf-SET readout is that it can easily be turned on and off, although for the measurements reported here it is operated in a continuous way.[10] More significantly, the rf-SET is fundamentally different from qubit readout based on switching currents in that it involves a weak measurement of the charge in contrast to a yes or a no answer. This could be a significant advantage for readout of multiple-qubit systems. For example, a switching current measurement on one qubit would also directly affect the other qubits due to its strong interaction. Furthermore, switching current measurements are inherently stochastic in time—an important consideration if one is interested in measuring time correlations.

Electron-beam lithography and double-angle shadow evaporation of aluminum films onto an oxidized silicon substrate were used to fabricate the combined SCB-SET system (see Fig. 1).[11] The SCB box consists of a low-capacitance superconducting island connected to a superconducting reservoir by two parallel junctions that define a low-inductance SQUID loop. An additional gate lead placed near the island is used to change the electrostatic potential of the island by a gate voltage V_g through a gate capacitance C_g. By adjusting the magnetic flux Φ through the loop, the effective Josephson energy is tunable as $E_J = E_J^{max}|\cos(\pi\Phi/\Phi_0)|$, where Φ_0 is the magnetic-flux quantum $(h/2e)$. Coupling of the SCB to the SET was accomplished by extending part of the SET island to the proximity of the box island and resulted in a weak dimensionless coupling, C_I/C_Σ of 0.5–4% for samples with slightly different geometries and total SCB capacitances C_Σ. C_I is the capacitance between the SCB and SET islands.

The samples were placed at the mixing chamber of a dilution refrigerator with a base temperature of ≈ 20 mK. An external superconducting magnet was used to produce a large field parallel to the plane of the samples and a small superconducting coil close to the sample was used to produce a

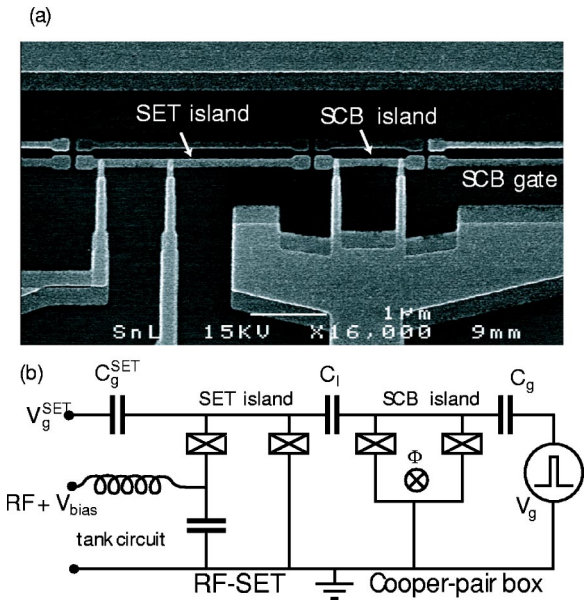

FIG. 1. (a) Scanning electron micrograph of a sample. The device consists of a Cooper-pair box and SET electrometer and was fabricated from an aluminum (lighter regions) evaporated onto an oxidized Si substrate (darker regions). (b) Circuit diagram of box and electrometer.

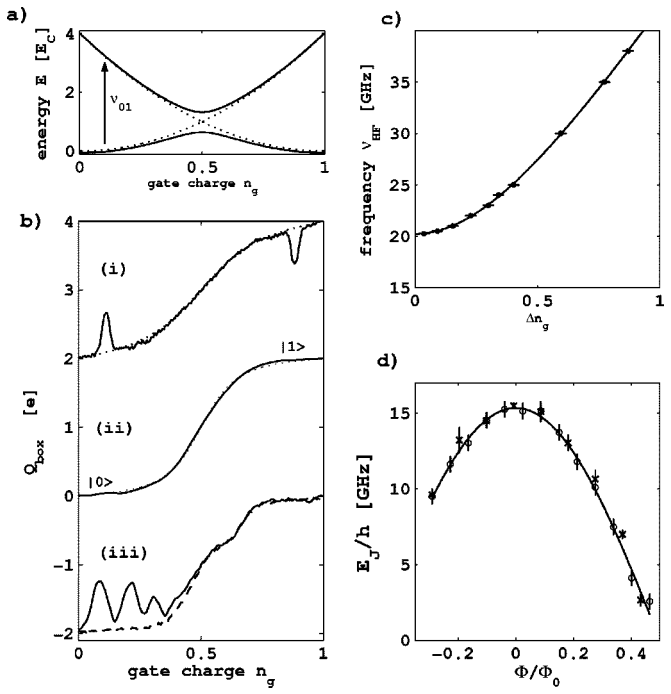

FIG. 2. (a) Ground-state and first excited-state energies vs n_g for $E_J/E_C=0.7$ (solid line) and $E_J=0$ (dotted line). (b) Coulomb staircases, Q_{box} versus n_g for a sample with $E_c/h=9.25\pm0.10$ GHz and $E_J^{max}/h=20.24\pm0.10$ GHz. In (i) a staircase taken from a sample under microwave radiation with a frequency of 35 GHz is shown. In (ii), we show data where E_J/h has been suppressed to 11.4 GHz by applying a small magnetic field through the SQUID loop. The dotted lines in (i) and (ii) show the calculated Q_{box} vs n_g for the respective Josephson energies. (iii) Measured Q_{box} vs n_g (solid line) when a fast pulse train is applied to the SCB gate having an amplitude $0.88e$, width $\Delta t=130$ ps, and repetition time $T_R=130$ ns (here $E_J/h=4$ GHz). The dashed line is the measured Q_{box} without the pulse train. (c) Avoided level crossing shown by the positions of the spectral peaks and dips, $\Delta n_g=(n_g^{dip}-n_g^{peak})/2$, for varying microwave frequency. (d) Josephson energy E_J vs applied flux Φ/Φ_0 through the SQUID loop determined from spectroscopic data (circles) and coherent oscillation data (crosses). This sample had $E_c/h=17.45\pm0.13$ GHz and $E_J^{max}/h=15.5\pm0.2$ GHz.

field perpendicular to the SQUID loop. This allowed us to independently suppress the superconducting gap of the aluminum film, and change the effective Josephson energy of the Cooper-pair box. All control lines were filtered by a combination of low-pass and stainless steel and copper-powder filters. To present sharp pulses to the SCB gate, a high-frequency coaxial line was used having 10 dB attenuation at 4.2 K and 20 dB at 1.5 K. The tank circuit had a resonant frequency of 380 MHz and the rf-SET electrometer was biased near a feature in the IV vs V_g^{SET} landscape known as the double Josephson quasiparticle peak,[12] such that the bias current through the SET was typically 200–300 pA. Under these conditions, the electrometer sensitivity for the combined SCB-SET system was found to be $50\times10^{-6}e/\sqrt{\text{Hz}}$ with a bandwidth of 10 MHz.

To make an artificial two-level system, the energy scales of the SCB must be chosen so that $k_BT<E_C$, $E_J>\Delta$, where E_C is the energy cost required to add a single electron to the island and is set by total capacitance of the island $E_C=e^2/2C_\Sigma$. If Δ is large enough compared to E_C, then the ground states will be even parity states that differ only by the average number of Cooper pairs on the island. The effective Hamiltonian of the box, including the Josephson coupling, is given by

$$H=4E_C\sum_n (n-n_g)^2|n\rangle\langle n| - \frac{E_J}{2}\sum_n (|n+1\rangle\langle n|+|n\rangle\langle n+1|), \quad (1)$$

where we define gate charge as $n_g=C_gV_g/2e-n_0$, and n_0 is the offset charge due to stray charges near the box. Figure 2(a) shows the ground-state and first excited-state energy bands calculated using the Hamiltonian in Eq. (1). On account of the $2e$ periodicity of the system, we limit the discussion to gate charge $0\leqslant n_g\leqslant1$.

In thermodynamic equilibrium, the actual quantity that determines the island parity is the even-odd free energy difference $\tilde{\Delta}(T)$, which differs from Δ due to entropic considerations.[13] Measurements were made for several different samples with Coulomb energies $E_C/k_B(E_C/h)$ ranging from 0.43 to 1.65 K (9–34 GHz) and E_J/E_C ratios of 0.4 to 2.25. Coloumb staircases were measured by slowly ramping the box gate charge (at a rate of $\sim40e/s$), and measuring the power reflected from the rf-SET tank circuit. Examples of the measured box charge $Q_{box}(n_g)$ is shown in Fig. 2(b). Our samples show $2e$ periodicity when $E_c/k_B<1$ K, well below the gap $\Delta/k_B=2.2$ K. For samples with larger E_c, the

staircases acquire an extra step around $n_g = 0.5$ due to poisoning by nonequilibrium quasiparticles.

The characteristic energies E_C and E_J^{max} of the SCB can be determined directly using microwave spectroscopy.[10] When monochromatic microwaves are applied to the SCB gate, resonant peaks and dips occur in the measured Q_{box} vs n_g staircase when the microwave photon energy matches with the energy-level splitting ν_{01} [see Fig. 2(b)]. As the microwave frequency is reduced, the positions of these peaks exhibit an avoided level crossing. Within the two-level approximation, the positions of the single-photon resonances depend on the applied frequency ν as $\Delta n_g = \sqrt{h^2\nu^2 - E_J^2}/8E_C$, where we used $\Delta n_g \equiv (n_g^{dip} - n_g^{peak})/2$. An example of such an avoided level crossing is shown in Fig. 2(c) where we have used least-squares fits to this equation to estimate the Coulomb and Josephson energies.

Measurements of time-resolved, coherent oscillations of the charge on the SCB are made by slowly ramping the SCB gate charge n_g as before, while applying fast (nonadiabatic) rectangular dc-voltage pulses of amplitude a in the form of a pulse train to the SCB gate. When n_g is far away from the charge degeneracy and a such that $n_g + a$ places the system at the charge degeneracy, the leading and trailing edges of each pulse act as successive Hadamard transformations. In between, the system coherently oscillates between charge eigenstates for a time Δt. The trailing edge of the pulse returns the gate charge to n_g with the system in a superposition of ground and excited states corresponding to the phase of the oscillation acquired during Δt. After the pulse, the excited-state component decays with a relaxation time T_1. The pulses are separated by a repetition time T_R, typically greater than T_1.

Since the staircase is acquired by ramping n_g on a time scale much slower than T_R, one measures an enhanced charge $\Delta Q_{box} = Q_{box}^{on} - Q_{box}^{off}$ that is time averaged over the pulse train and proportional to the probability of finding the system in the excited state. Peaks in ΔQ_{box} vs n_g will be located at gate charges n_g^{peak} such that approximately a half-integer number of oscillations occur at gate charge $n_g^{peak} + a$ during the time Δt. Figure 2(b) (bottom curve) shows a measured staircase using such a pulse train. When one measures such staircases for varying Δt, then time-domain oscillations are evident in the Δt cross sections of ΔQ_{box} vs n_g. This is shown in Fig. 4(a), where we plot the time evolution near the charge degeneracy point. As T_R is increased, the pulse-induced charge contributes less to the time average. A simple calculation which ignores coherence effects remaining after a time T_R leads to the dependence

$$\Delta Q_{box}(T_R) = 2n_0 \frac{T_1}{T_R} \frac{1 - e^{-T_R/T_1}}{1 + e^{-T_R/T_1}}, \tag{2}$$

where n_0 is the initial peak amplitude. One can estimate T_1 at the readout gate voltage by measuring the dependence of the peak amplitude on T_R and fitting the data to this formula.

Using such a pulse-train allows a measurement of the excited-state probability even when the relaxation time T_1 is shorter than the measurement time. Population averaging and mixing limit the maximum observed amplitude of the ΔQ_{box} oscillations to $1e$ rather than $2e$, and this occurs only for an ideal rectangular pulse, short repetition times, and vanishing E_J/E_C ratio. We have numerically integrated the Schrödinger equation using pulses with a finite rise time to study the various factors affecting both the contrast of the oscillations and the degree of charge state polarization. The results are best understood when plotted on the Bloch sphere as shown in Fig. 3. The dash-dotted lines show the evolution in time of the state vector starting from an initial condition (upward pointing arrows) and evolving through a maximum polarization of the charge state (downward arrows). The initial state differs from pure $\mathbf{S}_z$ due to a finite E_J/E_C. Figure 3(a) shows evolution for a pulse that takes the system to the charge degeneracy. One finds that a finite pulse rise time mimics a higher E_J/E_C ratio and reduces the oscillation contrast. Nonetheless, Fig. 3(b) shows that by pulsing past the charge degeneracy, one can achieve nearly 100% polarization.

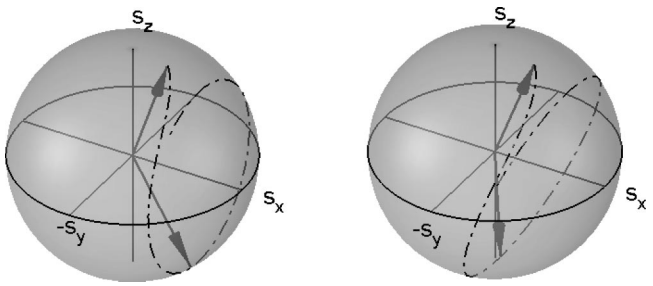

FIG. 3. (a) Bloch sphere showing evolution about the charge degeneracy for $E_J/h = 6$ GHz, $E_C/h = 9$ GHz, and a pulse rise time of 35 ps. (b) Evolution for a pulse that takes the system past the charge degeneracy and achieves 100% charge state polarization (downward pointing arrow).

Measurements of the T_R dependence of ΔQ_{box} are shown in Fig. 4(b), where we have used an appropriate pulse amplitude and duration to achieve nearly 100% initial polarization. We find $T_1 = 108 \pm 20$ ns at the readout point $n_g \simeq 0.25$ using a least-squares fit to Eq. (2). The data of Fig. 4(a) show an oscillation contrast of $\approx 0.55e$. Taking into account the experimentally determined E_J/E_C and T_1/T_R, along with the measured rise time $\delta t \simeq 35$ ps of our pulse generator (Anritsu MP1763C), we find good agreement between the observed and expected initial oscillation contrast. Numerical solutions of Schrödinger equation show that the reduction of contrast due to the pulse rise time depends strongly on E_J. This was checked experimentally by varying E_J and found to be in agreement with the calculations. A fit of the data of Fig. 4(a) to an exponentially decaying sinusoid gives an oscillation frequency $\nu_0 = 3.6$ GHz and decoherence time of 2.9 ns.

Using fast dc pulse trains we were able to observe oscillations in time out to 10 ns. The dependence of decoherence time on gate charge at the top of the pulse is shown in Fig. 4(c) and has a sharp maximum at the charge degeneracy. This tells us that low-frequency charge noise is the dominant source of dephasing in our qubit. As discussed and demonstrated by Vion *et al.*,[2] dephasing due to charge fluctuations is minimum at the charge degeneracy. The coherence time

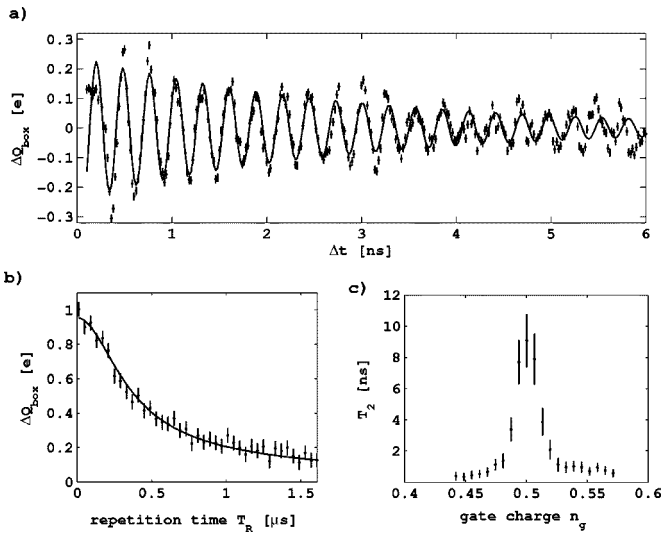

FIG. 4. (a) ΔQ_{box} vs Δt. The solid line is a least-squares fit to an exponentially decaying sinusoid and gives a decay time $T_2 \simeq 2.9$ ns and frequency $\nu_0 = 3.6$ GHz. (b) Dependence of the peak height ΔQ_{box} on repetition time T_R for $\sim 100\%$ initial polarization. The solid line is a least-squares fit to Eq. (2) giving $T_1 = 108 \pm 20$ ns. (c) Decoherence time T_2 vs gate charge n_g.

found by Vion *et al.* is much larger than that found in our measurements although their initial oscillation amplitude is much smaller. If we extrapolate the gate charge dependence of T_1 (not shown) to the charge degeneracy, we expect $T_1 \sim 10$ ns. This implies that the decoherence time we measure at the charge degeneracy is dominated by the short relaxation time rather than pure dephasing.

Our measured T_1 was also found to be independent of SET bias current in the subgap regime. Previously, a considerably larger T_1 was measured in a similar sample using a spectroscopic technique,[10] and found to agree with the theoretical $T_1 \simeq 1\ \mu s$ expected from quantum fluctuations of a 50 Ω environment. The reduced T_1 observed here could be attributed to several factors. One is coupling to the relatively unfiltered high-frequency coaxial line, in addition to unwanted coupling to other metal traces and the microwave environment of our sample. In practice it is difficult to estimate the actual real part of the impedance on these leads at such high transition frequencies. Another possibility concerns quasiparticles. Our samples were fabricated without quasiparticle traps and despite the observed static $2e$ periodicity, there could be considerable nonequilibrium quasiparticle dynamics occurring on these time scales. Finally, it may be that the use of fast dc pulses leaves the bath of charge fluctuators in a configuration having additional channels for relaxtion of the qubit. Clearly what is needed is T_1 measurements using a variety of techniques—rf rotations, spectroscopy, as well as fast dc pulse—on the same sample.

In conclusion, we have fabricated and measured a solid-state qubit based upon a SCB combined with a rf-SET readout system. Due to a relatively short T_1, continuous measurement of the SCB was employed. Fast dc pulses were used to coherently manipulate the qubit and time-coherent oscillations of the charge were observed. The initial contrast of the oscillations is relatively large and quantitatively understood as due to finite E_J/E_C combined with the finite pulse rise time. Furthermore, nearly 100% charge state polarization can be achieved. The oscillations show a maximum decoherence time at the charge degeneracy which indicates that charge fluctuations dominate the dephasing rate.

We would like to acknowledge fruitful discussions with R. Schoelkopf, K. Lehnert, A. Wallraff, G. Johansson, A. Käck, G. Wendin, and Y. Nakamura. The samples were made at the MC2 clean room. The work was supported by the Swedish SSF and VR, by the Wallenberg and Göran Gustafsson foundations, and by the EU under the IST-SQUBIT programme.

*Electronic address: tim@mc2.chalmers.se

[1] Y. Nakamura, Y.A. Pashkin, and J.S. Tsai, Nature (London) **398**, 786 (1999).
[2] D. Vion, A. Aassime, A. Cottet, P. Joyez, H. Pothier, C. Urbina, D. Esteve, and M.H. Devoret, Science **296**, 886 (2002).
[3] C.H. van der Wal *et al.*, Science **290**, 773 (2000).
[4] I. Chiorescu, Y. Nakamura, C.J.P.M. Harmans, and J.E. Mooij, Science **299**, 1869 (2003).
[5] Y. Yu, S. Han, X. Chu, S.-I. Chu, and Y. Wang, Science **296**, 889 (2002).
[6] J.M. Martinis, S. Nam, J. Aumentado, and C. Urbina, Phys. Rev. Lett. **89**, 117901 (2002).
[7] R.J. Schoelkopf, P. Walgren, A.A. Kozhevnikov, P. Delsing, and D.E. Prober, Science **280**, 1238 (1998).
[8] A. Aassime, D. Gunnarsson, K. Bladh, and P. Delsing, Appl. Phys. Lett. **79**, 4031 (2001).
[9] A. Aassime, G. Johansson, G. Wendin, R.J. Schoelkopf, and P. Delsing, Phys. Rev. Lett. **86**, 3376 (2001).
[10] K.W. Lehnert, K. Bladh, L.F. Spietz, D. Gunnarsson, D.I. Schuster, P. Delsing, and R.J. Schoelkopf, Phys. Rev. Lett. **90**, 027002 (2003).
[11] K. Bladh *et al.*, Phys. Scr. **T102**, 167 (2002).
[12] A.A. Clerk, S.M. Girvin, A.K. Nguyen, and A.D. Stone, Phys. Rev. Lett. **89**, 176804 (2002).
[13] P. Lafarge, P. Joyez, D. Esteve, C. Urbina, and M.H. Devoret, Nature (London) **365**, 6445 (1993).